Shot repetition

An alternative seismic blending code in marine acquisition

Wu, Sixue; Blacquière, Gerrit; Adriaan Van Groenestijn, Gert Jan

Important note
To cite this publication, please use the final published version (if applicable).
Please check the document version above.

Check for updates

Shot repetition: An alternative seismic blending code in marine acquisition

Sixue Wu[1], Gerrit Blacquière[2], and Gert-Jan Adriaan van Groenestijn[3]

ABSTRACT

In blended seismic acquisition, or simultaneous source seismic acquisition, source encoding is essential at the acquisition stage to allow for separation of the blended sources at the processing stage. In land seismic surveys, the vibroseis sources may be encoded with near-orthogonal sweeps for blending. In marine seismic surveys, the sweep type of source encoding is difficult because the main source type in marine seismic exploration is the air-gun array, which has an impulsive character. Another issue in marine streamer seismic data acquisition is that the spatial source sampling is generally coarse. This hinders the deblending performance of algorithms based on the random time delay blending code that inherently requires a dense source sampling because they exploit the signal coherency in the common-receiver domain. We have developed an alternative source code called shot repetition that exploits the impulsive character of the marine seismic source in blending. This source code consists of repeated spikes of ones and can be realized physically by activating a broadband impulsive source more than once at (nearly) the same location. Optimization of the shot-repetition type of blending code was done to improve the deblending performance. As a result of using shot repetition, the deblending process can be carried out in individual shot gathers. Therefore, our method has no need for a regular dense source sampling: It can cope with irregular sparse source sampling; it can help with real-time data quality control. In addition, the use of shot repetition is beneficial for reducing the background noise in the deblended data. We determine the feasibility of our method on numerical examples.

INTRODUCTION

Blended acquisition, also known as simultaneous source acquisition, has become increasingly popular because it can achieve a higher data quality and/or better economics (Beasley et al., 1998; Berkhout, 2008). There are two main strategies of dealing with the blended data. One is to separate the blended data as if they were acquired conventionally before imaging (e.g., Mahdad et al., 2011; Zu et al., 2017). The other is to directly image the blended data (e.g., Verschuur and Berkhout, 2011; Dai et al., 2012; Soni and Verschuur, 2014; Chen et al., 2017). In this work, the former strategy is investigated to suit the current standard industrial processing needs.

For the past 50 years, source-encoding techniques have been developed to speed up data acquisition that achieves a dense spatial sampling (Barbier and Viallix, 1973; Bernhardt and Peacock, 1978; Womack et al., 1990). In seismic exploration, we are dealing with two types of source signatures: short-duration impulsive and long-continuous sweep (Ikelle, 2010). The sweep type of source-encoding techniques, especially the linear sweep for onshore vibroseis applications, has been well-developed. In land vibroseis surveys, multiple sources that release sweep signals are recorded simultaneously (e.g., Andersen, 1995; Bagaini, 2006). Many of the vibroseis sweeps are designed based on the orthogonality of signals; i.e., the autocorrelation of each signal is spiky, whereas the crosscorrelation of the signals is minimum. Such simultaneously acquired data can be separated as if they were acquired in a conventional way in the processing stage (Bagaini, 2008). The sweep type of source encoding cannot be applied to the air-gun array. In the current blended towed-streamer acquisition, mainly random time delays as a phase-encoding technique are applied to the impulsive air-gun sources along the source

[1]Delft University of Technology, Section of Applied Geophysics and Petrophysics, Department of Geotechnology, Faculty of Civil Engineering and Geosciences, PO Box 5048, 2600 GA Delft, The Netherlands. E-mail: s.wu@tudelft.nl.
[2]Delft University of Technology, Section of Applied Geophysics and Petrophysics, Department of Geotechnology, Faculty of Civil Engineering and Geosciences, PO Box 5048, 2600 GA Delft, The Netherlands and TNO Netherlands, PO Box 96864, 2509 JG The Hague, The Netherlands. E-mail: gerrit_blacquiere@hotmail.com.
[3]TNO Netherlands, PO Box 96864, 2509 JG The Hague, The Netherlands. E-mail: gert-jan.vangroenestijn@tno.nl.

inline direction (e.g., Vaage, 2002). The corresponding deblending method is effective; however, its performance is often hindered by sparse source sampling because the method inherently requires a dense source sampling as it exploits signal coherency when resorting to other domains such as the common-receiver domain. In this paper, we discuss a phase source encoding technique that enables deblending independent of source sampling. Other types of source-encoding techniques, such as the periodic source codes that involve time and space (e.g., Robertsson et al., 2016; Zu et al., 2016) and the source-encoding technique for the marine vibrator source (e.g., Halliday et al., 2017), are out of the scope of this paper. Similar to the vibroseis sweeps, the near-orthogonal marine source encoding can help in achieving goals such as enhancing the signal and separating the interference. Barbier and Viallix (1973) introduce the marine seismic acquisition method called Sosie, where the source energy is split into a sequence of discrete pulses that have a spiky autocorrelation function. This approach was proposed to replace dynamite sources such that the marine seismic acquisition would be more environmentally friendly. Abma et al. (2015) present the independent simultaneous source acquisition, which makes use of orthogonal properties in blended seismic acquisition. Individual air guns in one broadband source are activated with controlled time delays to form near-orthogonal sequences. This type of source encoding in a blended experiment allows effective deblending based on deconvolution of the source signature by sparse inversion in the common-source domain (Mueller et al., 2015). On the other hand, it imposes challenges on hardware and real-time seismic data quality control.

We present an alternative seismic blending code that exploit the impulsive character of the marine air-gun source and has no restrictions on source sampling (Wu et al., 2015). This source code, which we refer to as shot repetition, is a time sequence consisting of repeated spikes of ones and can be realized physically by activating the entire air-gun array or several identical subarrays more than once at (nearly) the same location. An iterative deblending method, which is adapted from the one used in Mahdad et al. (2011), has been implemented for deblending in individual shot gathers. It overcomes the sampling restrictions and simplifies real-time data quality control. Compared with the more orthogonal blending codes that require precise control of the individual air guns, the practical implementation of our method and subsequent real-time data quality control are more straightforward. Optimization of the shot-repetition type of blending code was done to improve the deblending performance.

In the following sections, we extend the general forward model of source blending to include the case of shot repetition. After explaining the deblending method, we show the results of deblending numerically blended field data with shot-repetition codes and a numerical example regarding background noise reduction. Finally, the deblending performance of the shot-repetition code is analyzed.

THEORY AND METHOD

Forward model

The matrix representation of seismic data (Berkhout, 1982) is used for constructing the forward model. The monochromatic seismic data are represented by $\mathbf{P}$, the so-called data matrix in the frequency domain. Each element of $\mathbf{P}$ is a complex-valued number that represents one frequency component of a recorded trace. Each column of $\mathbf{P}$ represents a monochromatic shot gather, and each row represents a monochromatic receiver gather. The general forward representation of source blending can be formulated as (Mahdad, 2012)

$$\mathbf{P}' = \mathbf{P}\boldsymbol{\Gamma}, \tag{1}$$

where P' is the blended data matrix and $\boldsymbol{\Gamma}$ is the matrix-blending operator that contains the blending codes. Each column of $\boldsymbol{\Gamma}$ corresponds to one blended seismic experiment, and each row of $\boldsymbol{\Gamma}$ corresponds to a source location. The concept of using shot repetition as a seismic blending code is a special case of the above general forward model. In the case of shot repetition, each source is activated more than once at nearly the same location. As a consequence, each nonzero element of the blending operator $\boldsymbol{\Gamma}$ leads to multiple time delays for the source at location k in blending experiment l. Hence, $\boldsymbol{\Gamma}_{kl}$ can be written as a sum of phase terms:

$$\Gamma_{kl} = \sum_{n=1}^{N} e^{-j\omega\Delta t_{kl,n}}, \tag{2}$$

where $\Delta t_{kl,n}$ is the time shift corresponding to the nth activation of the source. For $N = 1$, each source is activated once with a certain time delay, representing conventional random time delay type of source encoding. The corresponding deblending method requires the full data set and the deblending power depends on the randomness of the shot time delays when resorting to other domains such as common-receiver gathers. For $N > 1$, each source is activated more than once, representing shot repetition. The corresponding deblending method works on individual blended shot gathers. In this paper, we show examples with only one blended shot gather. In this case, the blending operator is a column of the full blending matrix $\boldsymbol{\Gamma}$ and the blended data are a column of the full blended data $\mathbf{P}'$ in equation 1. For deblending a full data set, all shot gathers can be processed separately.

A simple numerical example of the forward model is illustrated in Figure 1. The unblended data are modeled as a fixed receiver spread with a spacing of 20 m. Two shots at lateral location 0.56 and 2.48 km are coded with a pair of two-repetition source codes and summed together to generate the blended data shown in Figure 1c. The shot-repetition codes used here are illustrated in Figure 2a and 2b, in which the time delays between repeated spikes are 0.16 and 0.24 s, respectively.

Deblending method

Pseudodeblending

Deblending aims at retrieving individual shots as if they were acquired conventionally. The deblending process is an underdetermined inverse problem, meaning that the blended data matrix $\mathbf{P}'$ has fewer columns than $\mathbf{P}$. To solve this inverse problem, the following objective function is minimized:

$$J = \|\mathbf{P}' - \mathbf{P}\boldsymbol{\Gamma}\|_2^2. \tag{3}$$

The general solution of the above least-squares minimization is referred to as the pseudodeblended data:

$$P_{ps} = \mathbf{P}'\boldsymbol{\Gamma}^+, \tag{4}$$

$$\boldsymbol{\Gamma}^+ = (\boldsymbol{\Gamma}^H\boldsymbol{\Gamma})^{-1}\boldsymbol{\Gamma}^H, \tag{5}$$

where $\boldsymbol{\Gamma}^+$ is the generalized pseudoinverse and $\boldsymbol{\Gamma}^H$ is the transposed complex conjugate or the Hermitian of the blending operator $\boldsymbol{\Gamma}$. The pseudodeblending procedure can be expressed as applying $\boldsymbol{\Gamma}\boldsymbol{\Gamma}^+$ to

P according to equation 1. Because the blending operator $\mathbf{\Gamma}$ contains the source codes in the frequency domain, $\mathbf{\Gamma}^H$ in equation 5 performs correlations and $(\mathbf{\Gamma}^H\mathbf{\Gamma})^{-1}$ in equation 5 is a diagonal matrix that scales the output amplitude to be minimum in the least-squares sense. Accordingly, the diagonal elements of $\mathbf{\Gamma}\mathbf{\Gamma}^+$ are the scaled autocorrelations of the source codes and the off-diagonal elements are the scaled crosscorrelations of the source codes in the frequency domain. Hence, the pseudodeblending process can be seen as the scaled correlations of the source codes with the blended shot gather.

As an example, Figure 2 illustrates the diagonal and the off-diagonal elements of $\mathbf{\Gamma}\mathbf{\Gamma}^+$ after inverse Fourier transform, as the time-domain correlations, for $\mathbf{\Gamma}$ that contains the shot-repetition codes used in Figure 1. The zero-phased spikes in the autocorrelations in Figure 2c and 2d are related to the desired signals in Figure 1d and 1e, whereas the crosscorrelation in Figure 2 is related to the interfering events in Figure 1d and 1e, which is also referred to as blending noise. The success in deblending lies in the signal-to-blending-noise ratio in the pseudodeblended data, which is related to the amplitude ratio of the spike to the cross terms. Figure 2 shows that the spike amplitude of 0.5 in the scaled autocorrelations in Figure 2c and 2d is higher than the maximum value of 0.2 among the cross terms in Figure 2e, yielding a ratio of 2.5.

Each column of the pseudodeblended data $\mathbf{P}\mathbf{\Gamma}\mathbf{\Gamma}^+$ is a pseudodeblended shot gather that contains the scaled autocorrelation of the shot and the crosscorrelation with the blended shot. It can be observed that the desired signals have higher amplitudes compared with their sidelobes and the blending noise in Figure 1d and 1e. This signal enhancement is due to the near-orthogonal source codes that are featured by a spiky autocorrelation function and low crosscor-

relation values (Mueller et al., 2016). This feature essentially allows deblending individual blended shot gathers.

Benefit of amplitude scaling in the case of shot repetition

In the case of the random time delay type of source encoding, each nonzero element of the blending operator $\mathbf{\Gamma}$ contains a single phase term. The amplitude term $(\mathbf{\Gamma}^H\mathbf{\Gamma})^{-1}$ in pseudodeblending has scalar values on the diagonal for all frequencies. The pseudodeblending can be expressed as multiplying with $(1/b)\mathbf{\Gamma}^H$, where b is a scalar value representing the number of blended shots in one experiment and $\mathbf{\Gamma}^H$ corrects the phases in the correlation process (Mahdad, 2012). The amplitude scaling of $1/b$ ensures that the energy in the pseudodeblended data and the energy in the blended data are equal, but it does not affect the amplitude ratio of the desired signal to the blending noise in the common-shot domain. Figure 3a shows the amplitude term for a range of frequencies for $b = 2$.

As discussed before, pseudodeblending in the case of shot-repetition source encoding as a correlation process can enhance the signal-to-blending-noise ratio in the common-shot domain. From a processing point of view, the amplitude term $(\mathbf{\Gamma}^H\mathbf{\Gamma})^{-1}$ maximizes this ratio in the least-squares sense for each frequency component. It is a periodic function of frequency. Figure 3b shows the amplitude term for a range of frequencies for a shot-repetition code with $N = 2$. Without the amplitude term, the magnitude of the spike in autocorrelation would be N times the magnitude of the sidelobes and the crosscorrelation would be $2N$ spikes of the value $1/2N$ as normal correlation process for optimized source codes. Figure 2f–2h shows
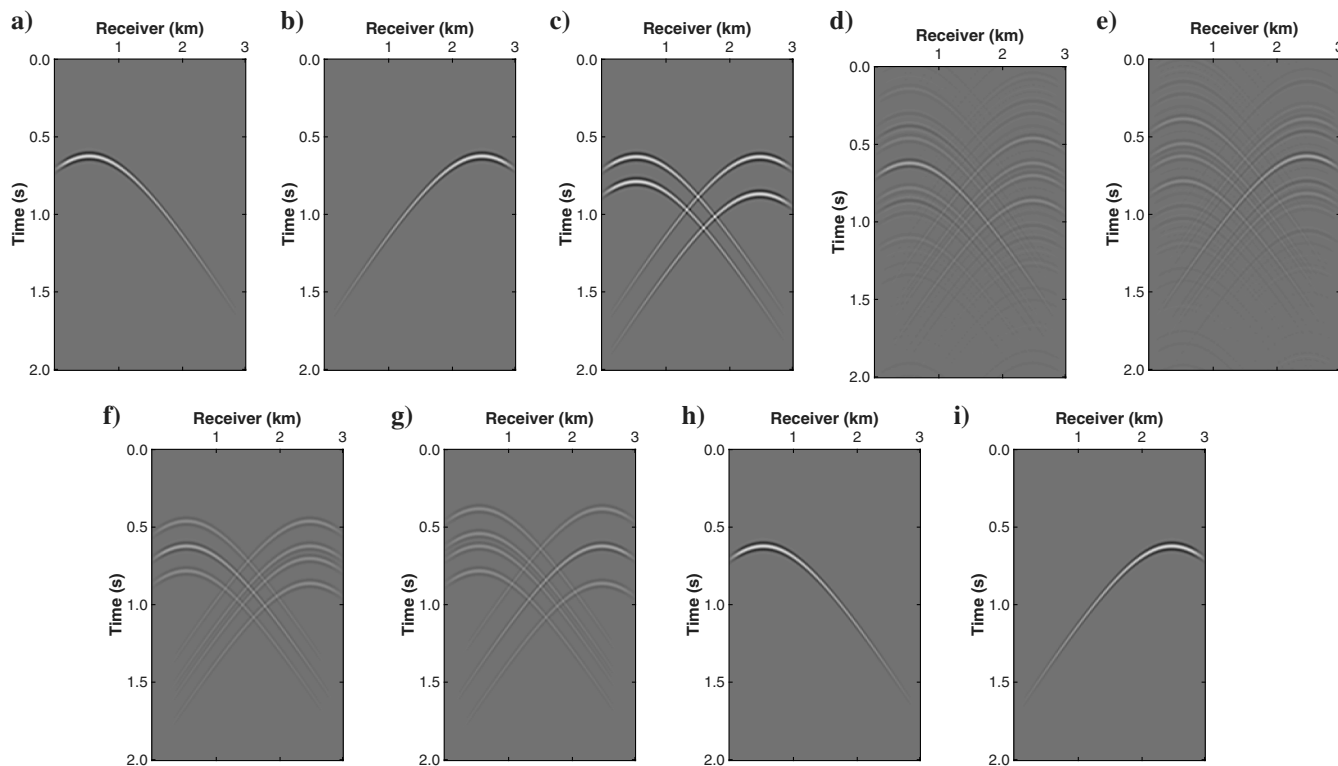

Figure 1. A numerical example of shot repetition: (a) unblended shot gather A, (b) unblended shot gather B, (c) blended shot gather, (d) pseudodeblended shot gather A, (e) pseudodeblended shot gather B, (f) correlated shot gather A, (g) correlated shot gather B, (h) deblended shot gather A, and (i) deblended shot gather B.

the correlations without the frequency-dependent amplitude scaling of the source codes in Figure 2a and 2b. Note that Figure 2f–2h is plotted with a scalar scale to compare with Figure 2c–2e. The ratio of the spike value to the maximum value of the cross terms is two, which is smaller than the one calculated before for Figure 2c–2e (2.5). In the least-squares sense, the ratio of the spike value in Figure 2f and 2g to

the sum of squared cross terms in Figure 2h is two. Whereas with amplitude scaling in pseudodeblending, it can be calculated that the spike value in Figure 2c and 2d versus the sum of squared cross terms in Figure 2e reaches a higher ratio of 3.28. As an example with the simple synthetic seismic data, Figure 1f and 1g shows the pseudodeblended shot gathers without the amplitude term. Note that Figure 1f and 1g is plotted with a scalar scale to compare with Figure 1d and 1e. It is clearly visible that the interferences in Figure 1f and 1g have higher amplitudes than the interferences in the pseudodeblended shot gathers with amplitude scaling shown in Figure 1d and 1e.

Iterative algorithm

To further reduce the blending noise from the pseudodeblended result, the iterative algorithm used in this paper is adapted from the deblending method proposed by Mahdad et al. (2011). That the deblending method is applicable in the common-shot domain is due to the fact that the desired signal is stronger than the interference in the pseudodeblended shot gathers. By incorporating a threshold for estimating the unblended data, we promote sparsity in the solution and the deblending problem is solved iteratively. The iterative updating scheme can be formulated as

$$\mathbf{P}^{i+1} = \mathbf{P}'\mathbf{\Gamma}^{+} - \bar{\mathbf{P}}^{i}[\mathbf{\Gamma}\mathbf{\Gamma}^{+} - \mathbf{I}], \qquad (6)$$

where $\mathbf{P}^{i+1}$ represents the deblending result at iteration $i + 1$, $\bar{\mathbf{P}}^{i}$ represents the deblended estimate constrained by the threshold at the ith iteration, and $\mathbf{I}$ is the identity matrix. A workflow of the deblending method in the case of shot repetition is given in Figure 4. The iterative process starts by applying a threshold to the pseudodeblended data $\mathbf{P}_{ps}$, yielding a deblended estimate $\bar{\mathbf{P}}^{i}$. This estimate is blended and pseudodeblended, and the interference is reconstructed by subtracting $\bar{\mathbf{P}}^{i}$ from $\bar{\mathbf{P}}^{i}\mathbf{\Gamma}\mathbf{\Gamma}^{+}$. The estimated interference $\bar{\mathbf{P}}^{i}[\mathbf{\Gamma}\mathbf{\Gamma}^{+} - \mathbf{I}]$ is subtracted from the pseudodeblended data $\mathbf{P}'\mathbf{\Gamma}^{+}$. The outcome is $\mathbf{P}^{i+1}$ containing less interfering energy. The iteration stops when there is no further improvement of the outcome. The results shown in Figure 1h and 1i are obtained by deblending the shot-repetition data in Figure 1c. It is clearly visible that the deblended shots are near-perfect compared with the original shots.

RESULTS

Field-data example

To test the feasibility of the proposed blending technique in a more realistic setting, we applied the deblending method to a numerically blended field data set. The original field data were from a 3D towed-streamer acquisition in the North Sea. The temporal and the spatial sampling interval are 4 ms and 12.5 m, respectively. In the preprocessed field data, the missing near offsets have been interpolated and reciprocity was used to convert the data from a towed-streamer geometry to a split-spread geometry (van Groenestijn, 2010). Two shot gathers at lateral locations 0.375 and 2.25 km
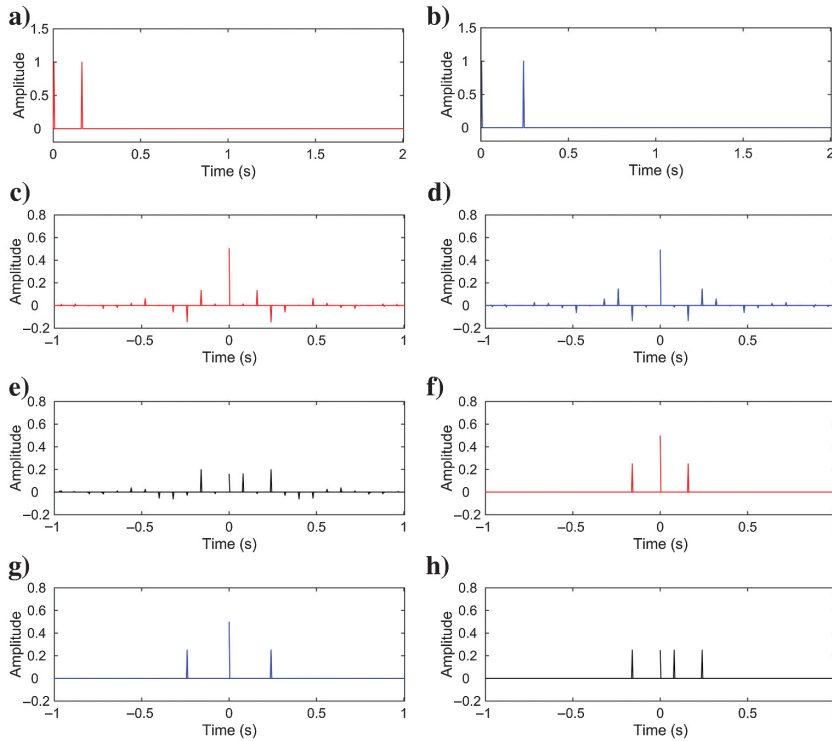

Figure 2. An illustration of a blending code set that contains two time delays: (a) source code A, (b) source code B, (c) scaled autocorrelation of source code A, (d) scaled autocorrelation of source code B, (e) scaled crosscorrelation of source codes A and B, (f) autocorrelation of source code A, (g) autocorrelation of source code B, and (h) crosscorrelation of source codes A and B.
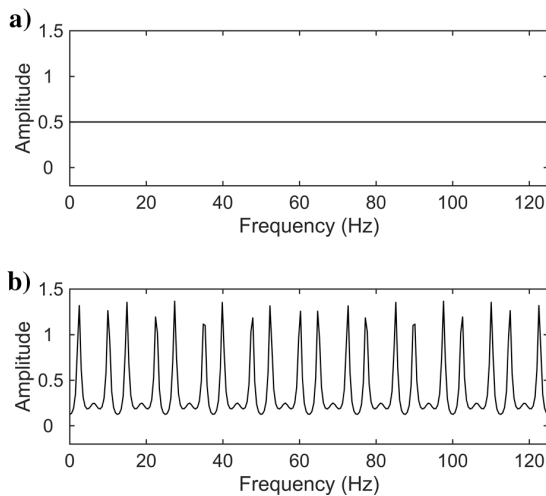

Figure 3. The amplitude terms of two blended sources, where (a) the source codes contain one time delay and (b) the source codes contain two time delays.

from the preprocessed field data are coded numerically with a pair of optimized source codes which consist of eight repetitions, and blended to generate the data shown in Figure 5a.

The pseudodeblended shot gathers are plotted in Figure 5b and 5f, and the final deblended shot records are plotted in Figure 5c and 5g. It is clear that the desired signal has a much higher amplitude than the blending noise after pseudodeblending. Compared with the original shot gathers in Figure 5d and 5h, it can be observed that the strong events in the shallow region from 0.0 to 1.2 s are well-resolved. The weak flat reflections in the deep region from 2.0 to 3.0 s are quite well-delineated. In this example, the deblending error can be computed and displayed because the field data were numerically blended. The deblending errors are plotted in Figure 5e and 5i. The signal-to-noise ratio of the deblended data is 10.2 dB; the signal-to-noise ratio of the pseudodeblended data is 3.1 dB; compared with the signal-to-noise ratio of the shot-repetition data (-11.8 dB), pseudodeblending reached an improvement of 14.9 dB and deblending reached an improvement of 22.0 dB. It took up to 10 s on a desktop computer to calculate the deblending results. This method can be easily paralleled for a full blended data set because the deblending process is carried out in individual blended shot gathers. This demonstrates that the technique can be applied during seismic acquisition and allows for real-time deblending quality control.

Noise reduction

Besides increasing the source density and/or reducing the survey time, blended acquisition improves the signal-to-noise ratio in seismic data (Berkhout and Blacquière, 2013). The blended and unblended marine seismic records contain the planned, man-made source signal as well as signals from other sources, such as traffic, fishing activities, flow noise, etc. The recorded events that are not related to the planned sources are referred to as the background noise. In the case of the shot repetition, more sources are used in each blended experiment and consequently more signal energy is sent into the subsurface, while the background noise remains the same. The signal-to-background-noise ratio in shot-repetition data is therefore more favorable compared with conventional data or regularly blended data without shot repetition. In Figure 6, random background noise that consists of f-k filtered spikes is simulated and added to numerical shot-repetition data, in which the unblended shot gathers in Figure 1a and 1b have been blended using the same set of source codes as in the field data example. After deblending, the results have a lower noise level with the signal-to-background-noise ratio being 4.5 dB (Figure 6c and 6d). The conventional data with the same noise have a signal-to-background-noise level of -5.8 dB. The improvement is 10.3 dB. Again, it is clear that the level of residual noise in the deblended results is lower than the initial background noise level.

Source-code optimization

An important aspect of blended acquisition is the source-code design. Mueller et al. (2016) describe a method for optimizing near-orthogonal source codes using a simulated annealing algorithm. Campman et al. (2017) use the so-called Golomb Ruler to optimize the shot-firing time in an algebraic way such that the correlation property is maximized. In the case of shot repetition, we use a trial-and-error algorithm to optimize the orthogonal properties of

the blending code, which means that we aim to obtain source code pairs with spiky autocorrelation and minimal crosscorrelation. The deblending power depends on the signal-to-blending-noise ratio after pseudodeblending. Because the pseudodeblended data can be seen as the convolution of the scaled correlations of the shot-repetition source codes (such as in Figure 2c and 2d) and the unblended data, the scaled correlations of a source code pair can be used to indicate deblending performance. The spikes in autocorrelations represent the signal, whereas the crosscorrelation represents the blending noise. The signal-to-blending-noise ratio in correlations can be evaluated by the amplitude of the spike in each autocorrelation divided by the sum of the squared crosscorrelation values. The number of parameters in our shot-repetition code optimization is $2N$, where N is the number of repetitions in equation 2. Because the number of repetitions is limited, the number of parameters is small. It takes only 0.2 ms on a desktop computer for one trial and the number of trials is user defined. Typically, several hundred pairs of optimized shot-repetition codes can be obtained after 10,000 trials.

Two pairs of source codes that contain eight repetitions are evaluated in Figure 7, where Figure 7a and 7c show the same source codes that have been applied to the field-data example in Figure 5a. The graphs on the left column correspond to the optimized source codes, whereas the graphs on the right column correspond to the nonoptimized source codes. In this comparison, the correlation graphs of the pair of nonoptimized source codes show sidelobes and cross terms with higher amplitudes than those calculated using the optimized codes. This indicates that blending with the optimized source codes can reach a better signal-to-blending-noise ratio than blending with the nonoptimized source codes in the pseudodeblended data.

Besides orthogonal properties, another factor that we considered in optimizing shot-repetition codes is the number of repetitions N. The larger the N value, the better the signal-to-blending-noise ratio in correlation and the better initial guess for deblending. This can be shown by comparing the scaled correlation graphs of the source codes, which contain two spikes in Figure 2, with the scaled correlation graphs of the source codes, which contain eight spikes in Figure 7.

Ten pairs of optimized source codes within a fixed time window are generated for each N that ranges from 2 to 8, and they are tested using the field data discussed above. The residual noise level shows a decreasing trend (Figure 8a). Furthermore, the signal-to-noise
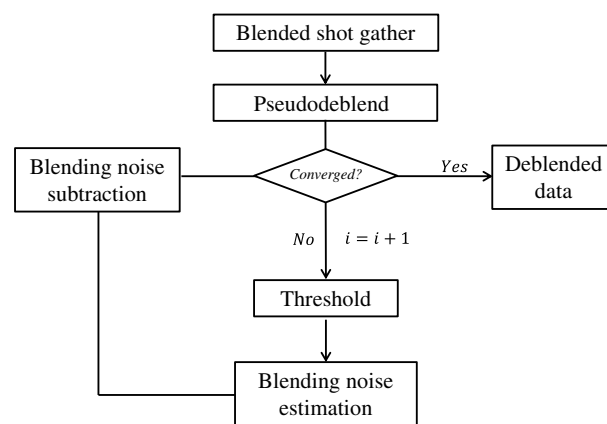

Figure 4. The workflow of the deblending method in the case of shot repetition.

ratio and the signal-to-noise-ratio improvement of the deblending results show an increasing trend (Figure 8b and 8c). This indicates that a higher number of shot repetitions is potentially better for the deblended data quality. Nevertheless, the residual noise level reduction with the increasing number of shot repetitions is limited. It is up to the acquisition requirement whether to adopt more repetitions in practice.

DISCUSSION

We have shown that the deblending method proposed by Mahdad et al. (2011) after a few modifications can be applied to

shot-repetition data in individual shot gathers. In this paper, a threshold as a simple sparsity constraint is chosen to test the feasibility of shot-repetition blending. A more sophisticated sparsity promoting procedure in the deblending algorithm such as the focal-curvelet hybrid transform (Kontakis and Verschuur, 2017) or a better denoising tool such as the rank-reduction method (Chen et al., 2016) would likely improve the results even further. Furthermore, it is convenient to combine shot-repetition codes with other blending codes because of the same general source-blending representation. Kontakis et al. (2016) perform numerical tests that combine shot repetition with the random time delays. The results showed that the additional constraints in the common-receiver
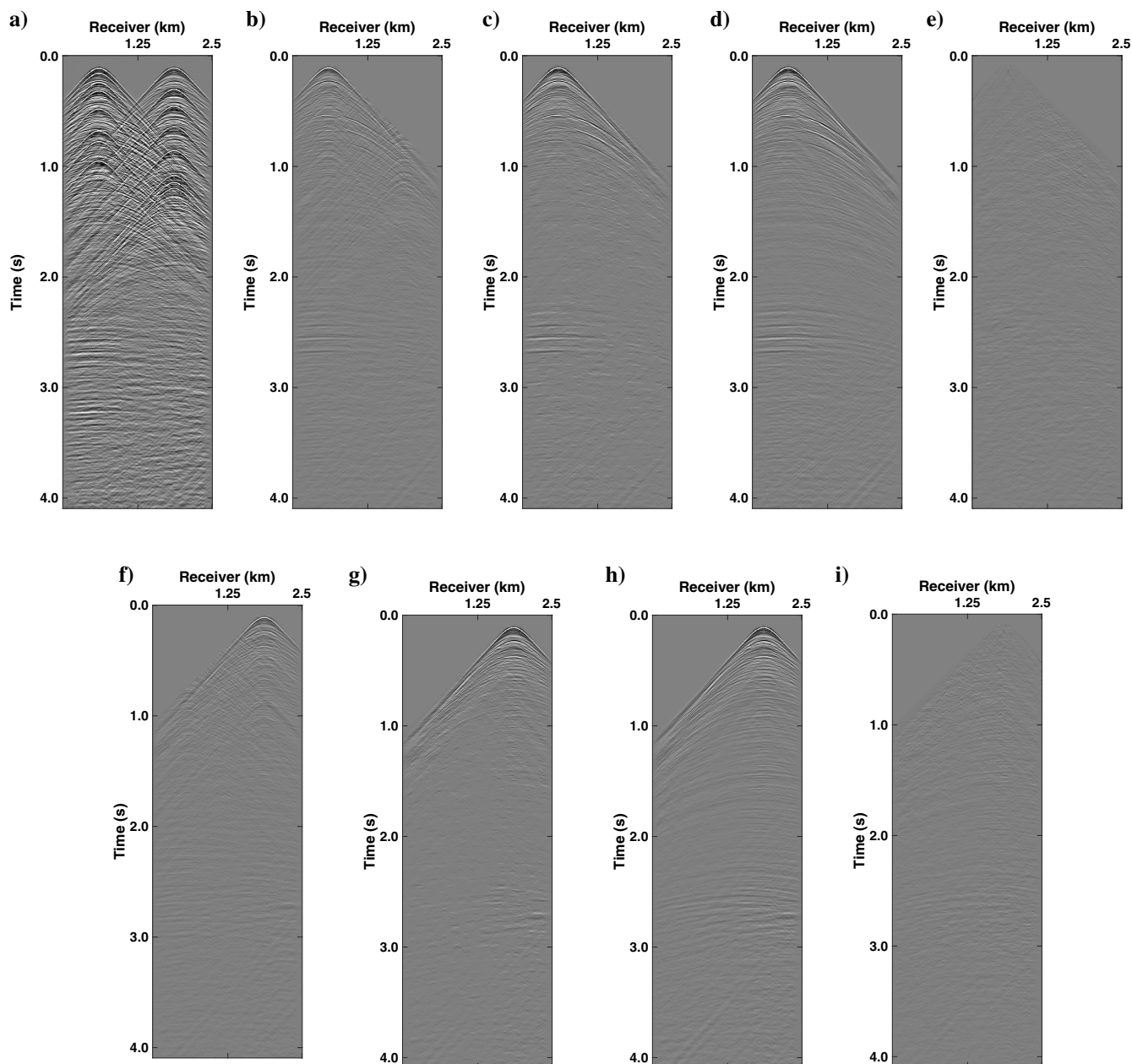

Figure 5. Field-data example: (a) numerically blended shot gather, (b) pseudodeblended shot gather A, (c) deblended shot gather A, (d) original shot gather A, (e) the deblending error of shot gather A (c-d), (f) pseudodeblended shot gather B, (g) deblended shot gather B, (h) original shot gather B, and (i) the deblending error of shot gather B (g-h).
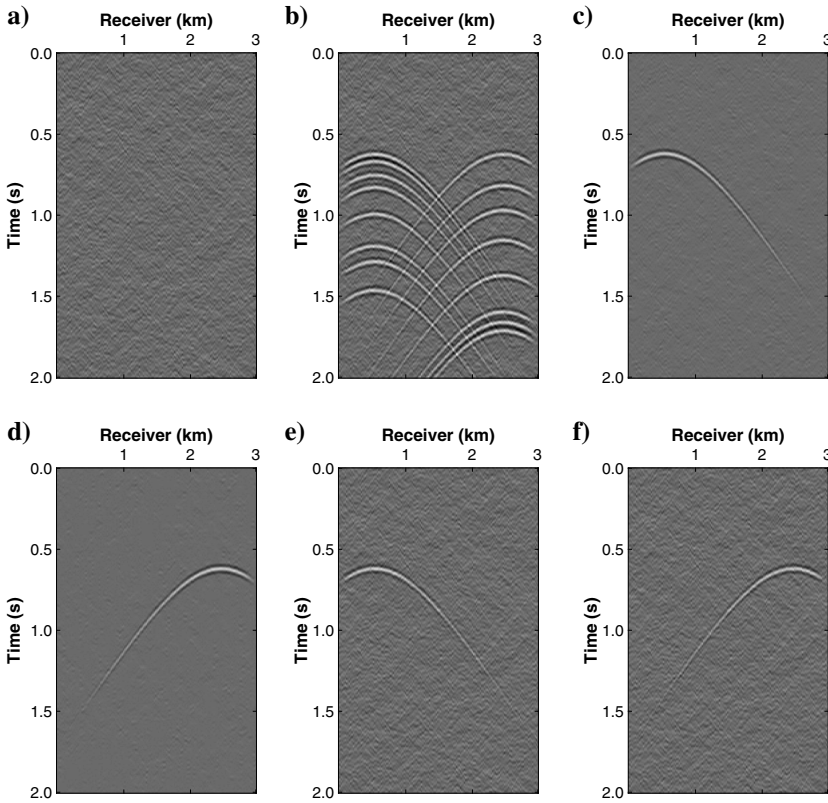
Figure 6. (a) Band-limited random background nosie, (b) blended shot gather with noise in (a), (c) deblended shot gather A, (d) deblended shot gather B, (e) conventional shot gather A with noise in (a), and (f) conventional shot gather B with noise in (a).
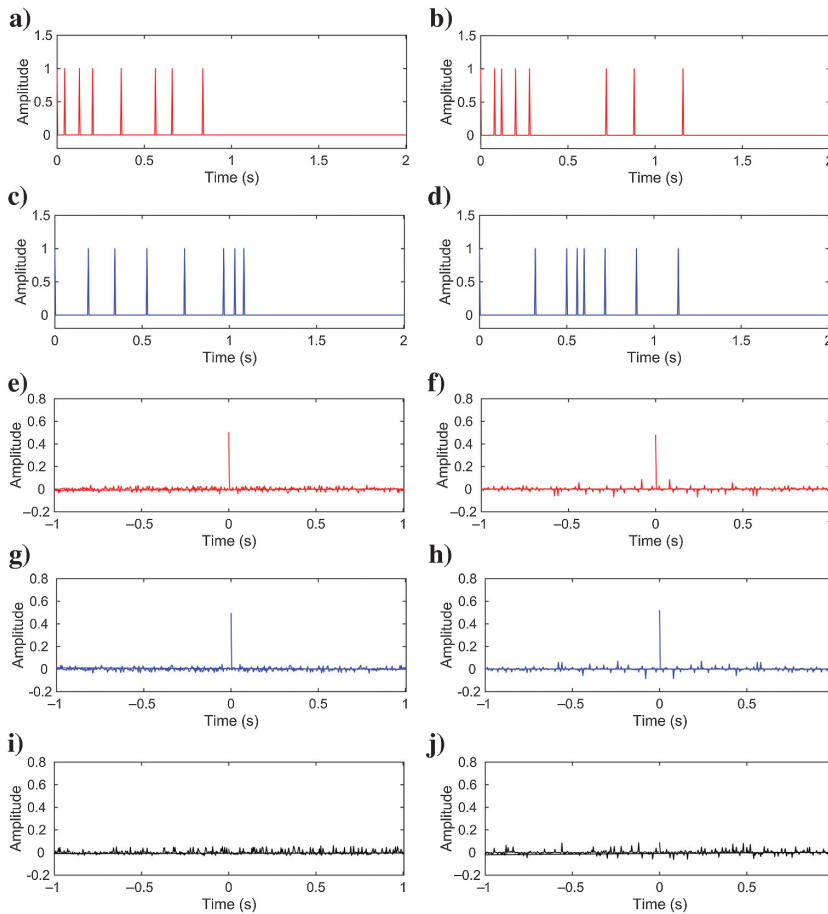

Figure 7. Left column: (a) optimized shot-repetition code A, (c) optimized shot-repetition code B, (e) scaled autocorrelation of source code A, (g) scaled autocorrelation of source code B, and (i) scaled crosscorrelation of source codes A and B. Right column: (b) nonoptimized shot-repetition code A, (d) nonoptimized shot-repetition code B, (f) scaled autocorrelation of source code A, (h) scaled autocorrelation of source code B, and (j) scaled crosscorrelation of source codes A and B.

domain can improve separating the interfering energy in deblending on the condition of a sufficiently dense source sampling. The deblending framework based on the shaping regularization proposed by Chen et al. (2014) offers a flexible way to control deblending using sparsity or coherency constraints. It is extended to a multiple-constraint regularized deblending framework by Chen (2015) with the extra constraint called iterative orthogonalization. From a processing point of view, this constraint enhances the signal-to-blending-noise ratio at each iteration and it helps to speed up the convergence.

As Abma and Ross (2015) address, practical aspects are important in seismic marine source encoding. Besides the optimization of source codes via evaluating correlation, some practical concerns should be addressed when designing such source codes, such as the varying source signatures, the engineering aspects, and the duration of the planned survey.

It has been shown that a larger repetition number N can potentially improve the deblending quality provided that each shot can be perfectly repeated. In practice, the signature varies from shot to shot. More repetitions could introduce more shot-by-shot signature variations due to higher operational uncertainties. The appropriate

choice of shot-repetition numbers in the code design should take the benefit and the operational uncertainties into account. The minimum time shift in source code design is restrained by many engineering aspects, e.g., the total capacity of the onboard compressors, the duration of refilling the air gun, and the bubble periods for different sizes of air guns. The maximum time shift is limited by the criterion that the duration of the blended survey has to be shorter than the duration of the corresponding unblended survey for economical reasons.

As mentioned before, the shot repetition type of source encoding can be realized in practice by activating the entire air-gun array or several identical subarrays in sequence (similar to Parkes and Hegna, 2011). Because the signature variation between the repeated shots at nearly the same source location is assumed to be identical in this theoretical study, we recommend measuring the firing times and the air-gun signatures to allow for successful deblending. In general marine applications of source encoding, the near-field hydrophone measurement of the source signatures is as important as the recording of the shot firing times for deblending such field data.

Moreover, the amplitude of all repeated shots may be reduced in the source-code design because the deblended data can still achieve the same amplitude as in the single-shot unblended data. This may contribute to a method that is more environmentally friendly with respect to the production of underwater noise. In a manner similar to that of the Sosie method proposed by Barbier and Viallix (1973), the energy of the output signal depends on the energy of the input signal. A prolonged input signal with lower average amplitude over time can supply the same amount of energy injection.

CONCLUSION

Shot repetition is a feasible alternative approach for source encoding in blended marine acquisition. It exploits the impulsive character of the marine seismic source. We demonstrated that the deblending method based on shot-repetition blending codes can be carried out in individual shot gathers with numerical blended field data. Accordingly, our method has no need for a regular dense source sampling: It can cope with sparse irregular source sampling; it can help with real-time data quality control. From the signal-to-noise ratio analysis of a range of optimized source codes, we showed that optimization of the source code can improve the deblending performance. Another benefit of incorporating more shots per source location is that it can help to reduce the random background noise.

It is possible to combine shot-repetition codes with other blending codes, e.g., random time delays to the blended inline sources. When the source sampling is sufficient, the additional constraint in other domains, such as the common-receiver domain, can improve separation of the interfering energy in deblending. When designing the source codes, it is beneficial to optimize them to improve the deblending performance. From a practical aspect, our source encoding method can be implemented straightforwardly by activating the entire air-gun array or several identical subarrays repetitively. Additional effort of real-time data quality control is minimum because the shot-repetition data resemble the conventional data appearing multiple times.
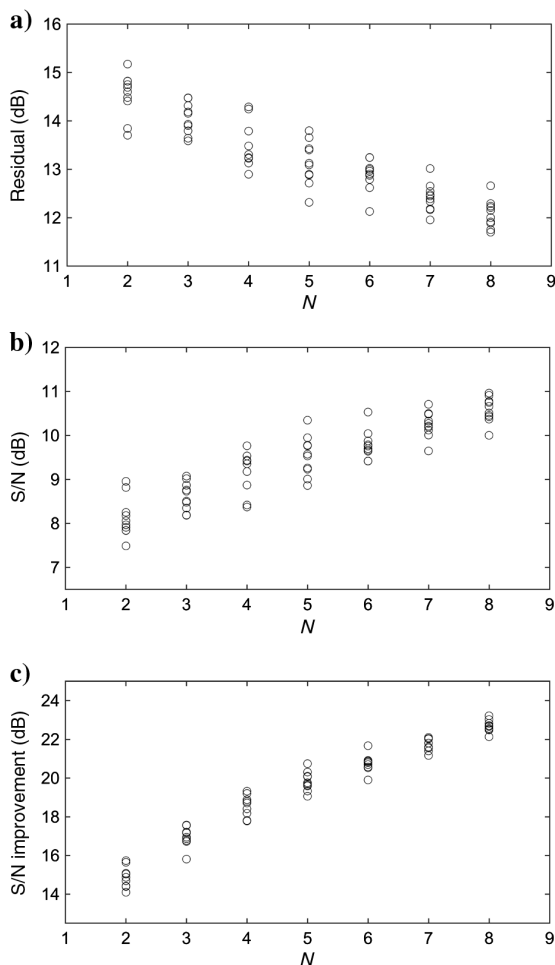
Figure 8. (a) The residual noise level in the deblending results. (b) The signal-to-noise ratio of the deblending results. (c) The signal-to-noise ratio improvement of the deblending results with increasing the number of shot repetitions.

discussions at the consortium meetings. PGS is acknowledged for permission to publish the field data. Y. Chen, A. Citlali Ramírez, Z. Tang, J. Shragge, and the anonymous reviewer are thanked for their suggestions that have improved the paper.

DATA AND MATERIALS AVAILABILITY

Data associated with this research are confidential and cannot be released.

REFERENCES

Abma, R., D. Howe, M. Foster, I. Ahmed, M. Tanis, Q. Zhang, A. Arogunmati, and G. Alexander, 2015, Independent simultaneous source acquisition and processing: Geophysics, **80**, no. 6, WD37–WD44, doi: 10.1190/geo2015-0078.1.

Abma, R., and A. Ross, 2015, Practical aspects of the popcorn source method: 85th Annual International Meeting, SEG, Expanded Abstracts, 164–169, doi: 10.1190/segam2015-5820723.1.

Andersen, K. D., 1995, Method for cascading sweeps for a seismic vibrator: U.S. Patent 5,410,517.

Bagaini, C., 2006, Overview of simultaneous vibroseis acquisition methods: 76th Annual International Meeting, SEG, Expanded Abstracts, 70–74, doi: 10.1190/1.2370358.

Bagaini, C., 2008, Vibroseis acquisition method: U.S. Patent 8,811,116.

Barbier, M. G., and J. R. Viallix, 1973, Sosie: A new tool for marine seismology: Geophysics, **38**, 673–683, doi: 10.1190/1.1440366.

Beasley, C. J., R. E. Chambers, and Z. Jiang, 1998, A new look at simultaneous sources: 68th Annual International Meeting, SEG, Expanded Abstracts, 133–135, doi: 10.1190/1.1820149.

Berkhout, A. J., 1982, Seismic migration, imaging of acoustic energy by wave field extrapolation, A: Theoretical aspects: Elsevier.

Berkhout, A. J., 2008, Changing the mindset in seismic data acquisition: The Leading Edge, **27**, 924–938, doi: 10.1190/1.2954035.

Berkhout, A. J., and G. Blacquière, 2013, Effect of noise in blending and deblending: Geophysics, **78**, no. 5, A35–A38, doi: 10.1190/geo2013-0103.1.

Bernhardt, T., and J. Peacock, 1978, Encoding techniques for the vibroseis system: Geophysical Prospecting, **26**, 184–193, doi: 10.1111/j.1365-2478.1978.tb01585.x.

Campman, X., Z. Tang, H. Jamali-Rad, B. Kuvshinov, M. Danilouchkine, Y. Ji, W. Walk, and D. Smit, 2017, Sparse seismic wavefield sampling: The Leading Edge, **36**, 654–660, doi: 10.1190/tle36080654.1.

Chen, Y., 2015, Iterative deblending with multiple constraints based on shaping regularization: IEEE Geoscience and Remote Sensing Letters, **12**, 2247–2251, doi: 10.1109/LGRS.2015.2463815.

Chen, Y., H. Chen, K. Xiang, and X. Chen, 2017, Preserving the discontinuities in least-squares reverse time migration of simultaneous-source data: Geophysics, **82**, no. 3, S185–S196, doi: 10.1190/geo2016-0456.1.

Chen, Y., S. Fomel, and J. Hu, 2014, Iterative deblending of simultaneous-source seismic data using seislet-domain shaping regularization: Geophysics, **79**, no. 5, V179–V189, doi: 10.1190/geo2013-0449.1.

Chen, Y., D. Zhang, Z. Jin, X. Chen, S. Zu, W. Huang, and S. Gan, 2016, Simultaneous denoising and reconstruction of 5-D seismic data via damped rank-reduction method: Geophysical Journal International, **206**, 1695–1717, doi: 10.1093/gji/ggw230.

Dai, W., P. Fowler, and G. T. Schuster, 2012, Multi-source least-squares reverse time migration: Geophysical Prospecting, **60**, 681–695, doi: 10.1111/j.1365-2478.2012.01092.x.

Halliday, D., R. Laws, and A. Ozbek, 2017, Phase sequencing, marine vibrators, and high multiplicity simultaneous sources: 87th Annual International Meeting, SEG, Expanded Abstracts, 57–61, doi: 10.1190/segam2017-17660035.1.

Ikelle, L., 2010, Coding and decoding: Seismic data: The concept of multishooting: Elsevier.

Kontakis, A., and D. Verschuur, 2017, Using a hybrid focal: Curvelet transform for deblending: 87th Annual International Meeting, SEG, Expanded Abstracts, 4903–4908, doi: 10.1190/segam2017-17671812.1.

Kontakis, A., S. Wu, and D. Verschuur, 2016, Acquisition geometry-aware focal deblending: 78th Annual International Conference and Exhibition, EAGE, Extended Abstracts, doi: 10.3997/2214-4609.201601411.

Mahdad, A., 2012, Deblending of seismic data: Ph.D. thesis, Delft University of Technology.

Mahdad, A., P. Doulgeris, and G. Blacquière, 2011, Separation of blended data by iterative estimation and subtraction of blending interference noise: Geophysics, **76**, no. 3, Q9–Q17, doi: 10.1190/1.3556597.

Mueller, M. B., D. F. Halliday, D. J. van Manen, and J. O. A. Robertsson, 2015, The benefit of encoded source sequences for simultaneous source separation: Geophysics, **80**, no. 5, V133–V143, doi: 10.1190/geo2015-0015.1.

Mueller, M. B., D. F. Halliday, D.-J. van Manen, and J. O. Robertsson, 2016, Optimizing near-orthogonal air-gun firing sequences for marine simultaneous source separation: Geophysics, **81**, no. 6, V415–V423, doi: 10.1190/geo2016-0197.1.

Parkes, G., and S. Hegna, 2011, A marine seismic acquisition system that provides a full 'ghost-free' solution: 81st Annual International Meeting, SEG, Expanded Abstracts, 37–41, doi: 10.1190/1.3627998.

Robertsson, J. O., L. Amundsen, and A. S. Pedersen, 2016, Signal apparition for simultaneous source wavefield separation: Geophysical Journal International, **206**, 1301–1305, doi: 10.1093/gji/ggw210.

Soni, A. K., and D. J. Verschuur, 2014, Full wavefield migration of vertical seismic profiling data: Using all multiples to extend the illumination area: Geophysical Prospecting, **62**, 740–759, doi: 10.1111/1365-2478.12130.

Vaage, S., 2002, Method and system for acquiring marine seismic data by using multiple sources: U.S. Patent 6,906,981.

van Groenestijn, G., 2010, Estimation of primaries and multiples by sparse inversion: Ph.D. thesis, Delft University of Technology.

Verschuur, D., and A. Berkhout, 2011, Seismic migration of blended shot records with surface-related multiple scattering: Geophysics, **76**, no. 1, A7–A13, doi: 10.1190/1.3521658.

Womack, J., J. Cruz, H. Rigdon, and G. Hoover, 1990, Encoding techniques for multiple source point seismic data acquisition: Geophysics, **55**, 1389–1396, doi: 10.1190/1.1442787.

Wu, S., G. Blacquière, and G. van Groenestijn, 2015, Shot repetition: An alternative approach to blending in marine seismic: 85th Annual International Meeting, SEG, Expanded Abstracts, 48–52, doi: 10.1190/segam2015-5858788.1.

Zu, S., H. Zhou, Y. Chen, S. Qu, X. Zou, H. Chen, and R. Liu, 2016, A periodically varying code for improving deblending of simultaneous sources in marine acquisition: Geophysics, **81**, no. 3, V213–V225, doi: 10.1190/geo2015-0447.1.

Zu, S., H. Zhou, W. Mao, D. Zhang, C. Li, X. Pan, and Y. Chen, 2017, Iterative deblending of simultaneous-source data using a coherency-pass shaping operator: Geophysical Journal International, **211**, 541–557, doi: 10.1093/gji/ggx324.